British Journal of Pharmacology

British Journal of Pharmacology (2017) **174** 2576–2590 2576

RESEARCH PAPER

The inward rectifier current inhibitor PA-6 terminates atrial fibrillation and does not cause ventricular arrhythmias in goat and dog models

Correspondence Marcel A G van der Heyden, Department Medical Physiology, DH&L, University Medical Center Utrecht, Yalelaan 50, 3584 CM Utrecht, The Netherlands. E-mail: m.a.g.vanderheyden@umcutrecht.nl

Received 5 December 2016; **Revised** 16 May 2017; **Accepted** 16 May 2017

Yuan Ji[1,*], Rosanne Varkevisser[1,*], Dragan Opacic[2,*], Alexandre Bossu[1], Marion Kuiper[2], Jet D M Beekman[1], Sihyung Yang[3], Azinwi Phina Khan[4], Dobromir Dobrev[4], Niels Voigt[4,5,6], Michael Zhuo Wang[3], Sander Verheule[2], Marc A Vos[1] and Marcel A G van der Heyden[1]

[1]Department of Medical Physiology, University Medical Center Utrecht, Utrecht, The Netherlands, [2]Department of Physiology, Cardiovascular Research Institute Maastricht, Maastricht, The Netherlands, [3]Department of Pharmaceutical Chemistry, School of Pharmacy, The University of Kansas, Lawrence, KS, USA, [4]Institute of Pharmacology, Faculty of Medicine, University Duisburg-Essen, Essen, Germany, [5]Institute of Pharmacology and Toxicology, University Medical Center Göttingen, Georg-August University Göttingen, Göttingen, Germany, and [6]DZHK (German Centre for Cardiovascular Research), Göttingen, Germany

*Authors contributed equally.

BACKGROUND AND PURPOSE

The density of the inward rectifier current (I_{K1}) increases in atrial fibrillation (AF), shortening effective refractory period and thus promoting atrial re-entry. The synthetic compound pentamidine analogue 6 (PA-6) is a selective and potent I_{K1} inhibitor. We tested PA-6 for anti-AF efficacy and potential proarrhythmia, using established models in large animals.

EXPERIMENTAL APPROACH

PA-6 was applied i.v. in anaesthetized goats with rapid pacing-induced AF and anaesthetized dogs with chronic atrio-ventricular (AV) block. Electrophysiological and pharmacological parameters were determined.

KEY RESULTS

PA-6 (2.5 mg·kg^{-1}·10 min^{-1}) induced cardioversion to sinus rhythm (SR) in 5/6 goats and prolonged AF cycle length. AF complexity decreased significantly before cardioversion. PA-6 accumulated in cardiac tissue with ratios between skeletal muscle : atrial muscle : ventricular muscle of approximately 1:8:21. In SR dogs, PA-6 peak plasma levels 10 min post infusion were 5.5 ± 0.9 μM, PA-6 did not induce significant prolongation of QTc and did not affect heart rate, PQ or QRS duration. In dogs with chronic AV block, PA-6 did not affect QRS but lengthened QTc during the experiment, but not chronically. PA-6 did not induce TdP arrhythmias in nine animals (0/9) in contrast to dofetilide (5/9). PA-6 (200 nM) inhibited I_{K1}, but not $I_{K,ACh}$, in human isolated atrial cardiomyocytes.

CONCLUSION AND IMPLICATIONS

PA-6 restored SR in goats with persistent AF and, in dogs with chronic AV block, prolonged QT intervals, without inducing TdP arrhythmias. Our results demonstrate cardiac safety and good anti-AF properties for PA-6.

Abbreviations

AERP, atrial effective refractory period; AF, atrial fibrillation; AP, action potential; cAVB, chronic atrio-ventricular block; CCh, carbachol; I_{K1}, inward rectifier K^+ current; LA, left atrium; LV, left ventricle; MAPD, monophasic action potential duration; PA-6, pentamidine analogue 6; QTc, heart rate-corrected ECG QT-interval; RA, right atrium; RV, right ventricle; SR, sinus rhythm; STV, short-term variability of repolarization duration; TdP, torsade de pointes

DOI:10.1111/bph.13869

Introduction

The inward rectifier K^+ current (I_{K1}) (Hibino *et al.,* 2010) is found in many excitable tissues, including the heart (De Boer *et al.,* 2010a). **I_{K1} channels** are composed of four $K_{ir}2.x$ subunits, either in a homo- or heteromeric configuration. In ventricles, **$K_{ir}2.1$** subunits are the major constituents, whereas in atria, $K_{ir}2.1$, **$K_{ir}2.2$** and **$K_{ir}2.3$** subunits are more equally contributing to functional channels (De Boer *et al.,* 2010a; Cordeiro *et al.,* 2015). Atrial cardiomyocytes have a 6- to 10-fold lower I_{K1} density than ventricular cardiomyocytes (Wang *et al.,* 1998; Cordeiro *et al.,* 2015). Nodal tissues lack functional I_{K1} (Satoh, 2003). Due to their conductive state around the potassium equilibrium potential and strong rectification behaviour, I_{K1} currents contribute to the resting membrane potential and its stability but allow proper action potential (AP) formation (Van der Heyden and Jespersen, 2016). Furthermore, the outward component of I_{K1} significantly contributes to phase 3 repolarization of the AP (Wang *et al.,* 1993; Biliczki *et al.,* 2002; Nagy *et al.,* 2013).

Atrial fibrillation (AF) is the most common arrhythmia observed in humans (Krijthe *et al.,* 2013). Clinically, AF is associated with increased risks for heart failure, stroke and death (Wolf *et al.,* 1991; Krahn *et al.,* 1995; Benjamin *et al.,* 1998). In a significant proportion of patients, AF progresses (Potpara *et al.,* 2012), as a result of electrical and structural atrial remodelling (Heijman *et al.,* 2014). Both processes increase the duration of AF episodes, a phenomenon known as 'AF begets AF' (Wijffels *et al.,* 1995). Electrical remodelling results in a shortened atrial effective refractory period (AERP) which facilitates atrial re-entry (Schotten *et al.,* 2011). Current guidelines indicate anticoagulation therapy and rate control or rhythm control (including catheter ablation) (Camm *et al.,* 2010, 2012), but the present treatment regimens often are inadequate (Gillis *et al.,* 2013), and, especially, rhythm control suffers from lack of efficacy and the occurrence of adverse effects, including cardiac proarrhythmia (Chinitz *et al.,* 2012). As I_{K1} densities increase in AF atria (Bosch *et al.,* 1999; Dobrev *et al.,* 2001, 2002) and may play a major role in AERP shortening (Zhang *et al.,* 2005), inhibitors of I_{K1} show potential as new drugs in the anti-arrhythmic pharmacotherapy repertoire (Ehrlich, 2008).

Starting with pentamidine for which we had demonstrated I_{K1} inhibiting capacity (De Boer *et al.,* 2010b), we selected a derivative, the pentamidine-analogue 6 (PA-6) with a highly favourable I_{K1} inhibiting profile (Takanari *et al.,* 2013). PA-6 inhibited both the inward and outward component of the current carried by $K_{ir}2.x$ with an IC_{50} of 12–15 nM for the different cardiac $K_{ir}2.x$ isoforms, as determined in the inside-out orientation of the patch-clamp method. Furthermore, in isolated canine ventricular cardiomyocytes, 200 nM PA-6 prolonged ventricular AP duration by 34%, without the occurrence of proarrhythmia. Finally, 200 nM of PA-6 did not affect $I_{Kv11.1}$, $I_{Kv7.1/MinK}$, $I_{Kv4.3}$, $I_{Ca,-L}$ or $I_{Nav1.5}$ (Takanari *et al.,* 2013).

In order to test the efficacy and safety of PA-6 *in vivo*, we used two established models in large animals, to avoid having to create and validate a single large animal model for both purposes. We used the goat model of AF induced by rapid atrial pacing (Wijffels *et al.,* 1995; Verheule *et al.,* 2013) and determined the effect of PA-6 infusion on the efficacy of cardioversion and on several electrophysiological parameters. To determine cardiac safety of PA-6, especially the absence of ventricular arrhythmias, we used the model of chronic AV block in dogs (Oros *et al.,* 2008). Furthermore, we determined the relation between PA-6 dosing and plasma and tissue concentration, as well as PA-6 plasma protein binding. Finally, we demonstrated that PA-6 is able to unmask the precise contribution of I_{K1} to inward rectifier K^+ current in human atrial cardiomyocytes.

Methods

Ethical statement

All animal care and management complied with the guidelines from Directive 2010/63/EU of the European Parliament. All animal experiments were approved by the Committee for Experiments on Animals of the Utrecht and Maastricht University, The Netherlands, for dog and goat experiments respectively. For human atrial cells, the study was approved by the local ethics committee of the University Duisburg Essen (No: 12–5268-BO), and each patient gave written informed consent. The investigation conforms with the principles outlined in the Declaration of Helsinki. Animal studies are reported in compliance with the ARRIVE guidelines (Kilkenny *et al.,* 2010; McGrath and Lilley, 2015). The current study has no implications for replacement, refinement or reduction.

Animal preparation and experiments

Goats. Eight female Dutch white milk goats weighing between 52.0 and 62.4 (56.7 ± 6.2) kg, age 16–24 (21.5 ± 2.6) months, obtained from a local farmer were used to evaluate the effect of PA-6 in an animal model of persistent AF. Goats were housed in pairs in conventional metal cages (approx. 8 m^2) on straw at a constant temperature and humidity with the 12 h light/dark cycle and free access to food (hay and pellets) and water. Animal welfare was checked daily, and body weight was measured once a week. All animals were instrumented with an atrial lead (Medtronic Capsurefix®) implanted transjugularly and fixed in the right atrial appendage. The pacemaker lead was connected to a subcutaneously implanted neurostimulator (Medtronic Itrel®). AF was induced and maintained by repetitive 50 Hz burst stimulation every other second, at four times the threshold, for 3 weeks (Verheule *et al.,* 2010).

Anaesthesia, both for implantation procedures and for follow-up experiments, was induced with sodium thiopental (20 $mg \cdot kg^{-1}$) and maintained with sufentanil (6 $\mu g \cdot kg^{-1} \cdot h^{-1}$) and propofol (10 $mg \cdot kg^{-1} \cdot h^{-1}$). In follow-up experiments, the muscle relaxant pancuronium bromide (Pavulon; 0.3- $mg \cdot kg^{-1} \cdot h^{-1}$) was added.

All animals ($n = 8$) underwent sacrifice experiment 3 weeks after the AF initiation, when electrical remodelling is complete without significant structural remodelling. Following termination of atrial pacing and anaesthesia induction, the heart was exposed through a left-sided thoracotomy. Subsequently the animals were allowed to

stabilize for 1 h. AF was considered as stable if it did not terminate spontaneously during this stabilization period.

Unipolar atrial electrograms were recorded with two custom-made high-density mapping electrodes (Ø 4 cm, 247 electrodes, interelectrode distance 2.4 mm) that were placed on the free walls of right and left atria. Electrograms were recorded with a custom-made 256 channel mapping amplifier (filtering bandwidth 0.1–408 Hz, sampling rate 1 kHz, A/D resolution 16 bits). The surface ECG was obtained from standard limb leads.

PA-6 (2.5 mg·kg^{-1}) was infused over 10 min as a bolus, followed by continuous infusion (0.04 mg·kg·min^{-1}) for 50 min. Blood samples were taken at baseline before drug infusion, after the PA-6 bolus administration (t = 10 min), and at 15, 20, 30, 40, 60, 70 and 90 min after the start of infusion. Skeletal muscle biopsies from the left hind limb were taken at baseline (before the start of PA-6 infusion), at end of the bolus administration and at 20 and 60 min after start of the infusion. Left ventricular (LV), right ventricular (RV), left atrial (LA) and right atrial (RA) tissues were harvested at the end of the experiment.

Surface ECG traces were analysed using IDEE-Q software (Instrument Development Engineering and Evaluation, Maastricht University, Maastricht, The Netherlands). QRS, RR and QT(c) intervals were analysed for 1 min periods at baseline, directly following the start of administration of the bolus, directly prior to and after cardioversion. The heart rate-corrected QT (QT_C) intervals were calculated by using the modified Bazett's formula $QTc = QT/(RR)^{0.6}$ according to Mohan *et al*. (2009).

For periods of 1 min, local atrial activation times were determined and fibrillation waves were reconstructed using custom-made analysis software (MATLAB 8.1, The Mathworks, Inc., Natick, Massachusetts, USA) as described before (Zeemering *et al.,* 2012; Lau *et al.,* 2015). AF complexity was quantified as the total number of waves and the number of breakthrough (BT) waves per AF cycle, mean wave size expressed as number of electrodes per wave, mean fractionation index defined as the ratio of subsidiary to dominant deflections and the mean wave conduction velocity (Duytschaever *et al.,* 2001; Eckstein *et al.,* 2011, 2013; Zeemering *et al.,* 2012; Lau *et al.,* 2015). All parameters were assessed at baseline (before PA-6 infusion), during the first minute of maintenance and during the last minute preceding cardioversion to sinus rhythm (SR).

Atrial fibrillation cycle length (AFCL) was calculated as median AFCL value during 60 s recordings, for both atria independently, and was assessed at three time points during stabilization period as a baseline, for every other minute during PA-6 infusion. The fifth percentile (p5) of the AFCL distribution was used as a surrogate parameter for the AERP during AF (Duytschaever *et al.,* 2001).

Dogs. A total of 10 adult mongrel dogs (7 females; 24.0 ± 2.3 kg; 2.6 ± 0.5 year; Marshall, New York, USA) were included in this study. Dogs were housed in pairs in conventional dog kennels (approx. 8 m^2) containing wooden bedding material. Animals had access to water *ad libitum* and received dog food pellets twice a day. Cages were enriched with playing tools, and animals were allowed to play in groups in an outdoor pen (50 m^2) once a day. Dogs were checked for comfort and health every day, and body weight was established once a week. Dose finding was performed during four experiments in four normal SR dogs. Yokoyama *et al*. (2009) infused pentamidine at 4 mg·kg^{-1}·40 min^{-1} in anaesthetized SR dogs resulting in a QTc increase of approximately 8% at 40 min. Given the 11-fold difference in I_{K1} IC_{50} values between pentamidine and PA-6 in inside-out measurements (Takanari *et al.,* 2013), we initially anticipated a PA-6 dose between 0.5 and 2.5 mg·kg^{-1} to be given in a period of 10–30 min that was subsequently adjusted to a period of 10 min. Arrhythmia inducibility by PA-6 and **dofetilide** was tested serially in nine chronic atrio-ventricular block (cAVB) dogs. AV block was induced by radiofrequency ablation, as described previously (Varkevisser *et al.,* 2013). In cAVB dog experiments, the animal was paced from the right ventricular apex at 60 bpm. All dog experiments were performed under general anaesthesia, which was induced with sodium pentobarbital (25 mg·kg^{-1} i.v.) and maintained by isoflurane (1.5% in O_2:NO_2 1:2). Premedication, pacing protocols and data analysis were as described previously (Varkevisser *et al.,* 2013). ECG parameters, monophasic action potentials (MAP) from left and right ventricular endocardial sites, were recorded.

PA-6 was dissolved in Milli-Q water and tested at two doses (0.5 and 2.5 mg·kg^{-1}). Before administration of PA-6, 10 min baseline was recorded. A continuous infusion of the low dose of PA-6 (0.5 mg·kg^{-1}) was given as a bolus during 10 min followed by an additional 20 min recording only period. Subsequently, the high dose of PA-6 (2.5 mg·kg^{-1}) was infused as a bolus over 10 min, and recordings were continued for another 20 min. Blood samples were collected before, directly after infusion of PA-6 and every 5 min during the measurement periods. In SR animals, awake ECG recordings were taken at regular intervals for up to 16 days. In cAVB dogs, dofetilide was applied at 0.025 mg·kg^{-1}·5 min^{-1} and recordings were continued for another 20 min. When torsade de pointes (TdP) arrhythmias were observed during the dofetilide infusion period, infusion was terminated immediately.

ECG data were recorded by the EPTracer program (Cardiotek, Maastricht, TheNetherlands). ECG parameters were quantified at baseline period and every 5 min after PA-6 administration. For each time point, RR, PQ, QRS and QT intervals were averaged from five successive beats. LV and RV monophasic APD at 80% repolarization (LV_{MAPD80} and RV_{MAPD80}) were analysed by MATLAB 8.3. Beat-to-beat variability of repolarization was quantified as short-term variability (STV) from 30 consecutive LV_{MAPD} recordings according to the formula $STV = \Sigma|D_{n+1} + D_n - 2D_{mean}|/[30 \times \sqrt{2}]$.

Dog cell isolation and patch clamp recordings. Experiments were all performed in adult ventricular cardiomyocytes (n = 8) isolated from two cAVB dogs (see above) using rupture patch configuration as described earlier (Takanari *et al.,* 2013). The isolation procedure has been already described previously (Nalos *et al.,* 2012). Patch clamp data were acquired and analysed with pCLAMP 10 software (Molecular Device, Sunnyvale, CA, USA).

Tissue binding assays and UPLC-MS/MS analysis. The binding of PA-6 to goat plasma and tissues was evaluated using rapid equilibrium dialysis devices (Thermo Scientific Pierce, Rockford, IL, USA) as previously described (Yang *et al.,* 2014). Thawed goat tissue samples were mixed with two volumes (vol/wt) of water (threefold dilution) and homogenized. Blank (untreated) plasma and tissue samples were taken from baseline period. PA-6 concentrations were determined as described below. For each sample, technical triplicates were used.

To prepare samples for ultra-performance liquid chromatography–tandem mass spectrometry (UPLC-MS/MS) analysis, plasma (5 μL), tissue homogenate (10 μL) or samples from tissue binding assays were mixed with 200 μL of 7:1 (vol/vol) methanol–water containing 0.1% trifluoroacetic acid and internal standard (20 nM pentamidine) and then vortex mixed for 30 s, followed by centrifugation (2800× *g*, 15 min) to pellet precipitated proteins. The supernatants were dried using a 96-well microplate evaporator (Apricot Designs Inc., Covina, CA, USA) under N_2 at 50°C and reconstituted with 150 μL 15% methanol containing 0.1% trifluoroacetic acid before UPLC-MS/MS analysis.

The reconstituted samples (2 μL injection volume) were analysed for drug concentration using a Waters Xevo TQ-S triple quadrupole mass spectrometer (Foster City, CA, USA) coupled with a Waters Acquity UPLC I-Class system. Compounds were separated on a Waters UPLC BEH C_{18} column (2.1 × 50 mm, 1.7 μm) equilibrated at 50°C. UPLC mobile phases consisted of water containing 0.1% (*v*/v) formic acid (A) and methanol containing 0.1% (*v*/v) formic acid (B). Analytical conditions for PA-6 and pentamidine were the same as those previously described for diamidines (Wenzler *et al.,* 2013). The characteristic multiple reaction monitoring transitions for PA-6 were *m/z* 492.3 → 372.3 (for quantification) and 492.3 → 196.1 (for confirmation), and the characteristic single reaction monitoring transitions for pentamidine was *m/z* 341.4 → 120.1, under positive electrospray ionization mode. The calibration curves for PA-6 ranged from 0.005 to 50 μM for plasma samples and from 0.1 to 100 μM for tissue homogenates. The interday coefficient of variation and accuracy were within ±15%.

Human atrial cardiomyocyte isolation and electrophysiological recordings. Right atrial appendages were obtained from 12 patients with SR. Atrial cardiomyocytes were isolated using a standard protocol (Voigt *et al.,* 2015), suspended in storage solution (mM: KCl 20, KH_2PO_4 10, glucose 10, K-glutamate 70, β-hydroxybutyrate 10, taurine 10, EGTA 10, albumin 1, pH = 7.4) and investigated within 6 h. Only well-striated, rod-shaped myocytes were used for current recordings.

Membrane currents were measured with standard whole-cell voltage-clamp technique (Dobrev *et al.,* 2005; Voigt *et al.,* 2010). Borosilicate glass microelectrodes had tip resistances of 2–5 MΩ when filled with pipette solution (in mM: K-aspartate 80, NaCl 8, KCl 40, Mg-ATP 5, EGTA 2, GTP-Tris 0.1, HEPES 10, pH = 7.4). Cardiomyocytes were superfused with a solution containing (in mM) NaCl 120, KCl 20, $MgCl_2$ 1, $CaCl_2$ 2, glucose 10, HEPES 10, pH = 7.4 at 22–24°C. Seal resistances were 4–8 GΩ. Series resistance and cell capacitance were compensated.

Drugs were applied *via* an additional rapid solution exchange system (ALA Scientific Instruments, Long Island, NY, USA). Data were not corrected for the calculated liquid junction potential (−12 mV, software JPCalc, version 2.2). To control for cardiomyocyte-size variability, the currents are expressed as densities (pA/pF).

Data and statistical analysis

The data and statistical analysis comply with the recommendations on experimental design and analysis in pharmacology (Curtis *et al.,* 2015). Groups were not randomized, and operators and data analysts were not blinded. Data were analysed using GraphPad Prism version 6.00 for Windows (GraphPad Software, La Jolla California USA). For normally distributed data, a Student *t*-test or ANOVA for paired samples with Tukey's HSD *post hoc* or Bonferroni correction for multiple comparisons were used, while non-parametric data were analysed using Wilcoxon rank-sum test and Friedman's test with Dunn's multiple comparison test. For human atrial cardiomyocytes differences between group, means were compared by unpaired Student's *t*-test. Results are presented as mean ± SD unless mentioned otherwise. Values of $P < 0.05$ were considered significant.

Materials

Dofetilide was supplied by Procter & Gamble Pharmaceuticals (Cincinnati, Ohio, USA). Other compounds were supplied as follows: isoflurane (Abbott Laboratories Ltd, Maidenhead, UK); PA-6 (ENDOTHERM GmbH, Saarbruecken, Germany); pancuronium bromide (Inresa Arzneimittel GmbH, Freiburg im Breisgau, Germany); propofol (Fresenius Kabi Nederland BV, Zeist, Netherlands); sodium thiopental (Rotexmedica GmbH, Trittau, Germany); sufentanil (Hameln Pharma Plus GmbH, Hameln, Germany).

Nomenclature of targets and ligands

Key protein targets and ligands in this article are hyperlinked to corresponding entries in http://www.guidetopharmacology.org, the common portal for data from the IUPHAR/BPS Guide to PHARMACOLOGY (Southan *et al.,* 2016), and are permanently archived in the Concise Guide to PHARMACOLOGY 2015/16 (Alexander *et al.,* 2015).

Results

PA-6 in the goat model of atrial fibrillation

Cardioversion success rate. At 3 weeks after AF induction, six of the eight goats (75.0%) were in stable AF (not terminating spontaneously for 60 min). Of these six goats, five animals cardioverted to SR during PA-6 infusion at the end of bolus (2.5 $mg \cdot kg^{-1} \cdot 10\ min^{-1}$) or briefly thereafter during maintenance (0.04 $mg \cdot kg^{-1} \cdot min^{-1}$) administration ($n$ = 5, 83%, Figure 1), with a mean time to cardioversion of 13.2 ± 4.9 min (6–19 min). The other animal cardioverted 11 min after the end of PA-6 infusion (71 min from start of

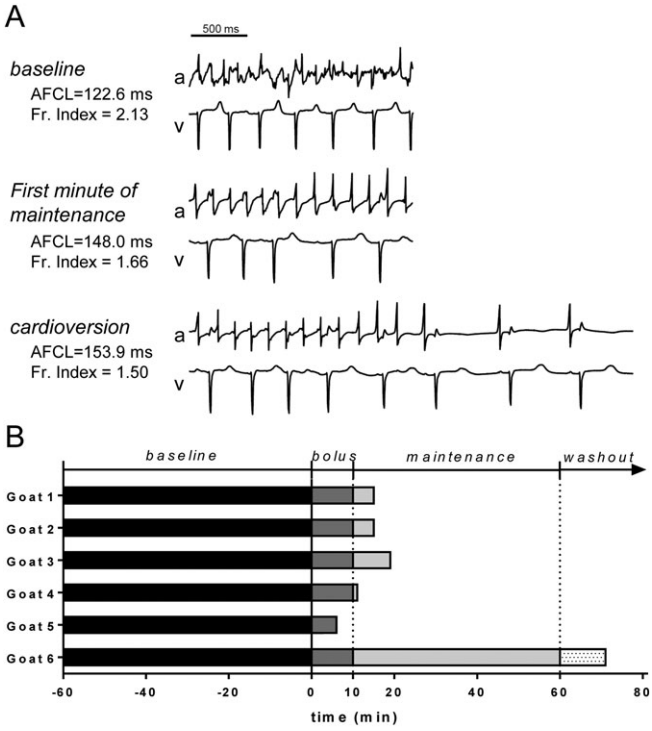

Figure 1

AF termination during PA-6 administration in goats with rapid pacing induced AF ($n = 6$). (A) Left atrial electrogram (a) and unipolar ventricular electrogram (v) recordings of goat #1 demonstrating AF and irregular ventricular rhythm (baseline), decrease in AF complexity (first minute of maintenance) and finally cardioversion resulting in SR (cardioversion). AFCL and fractionation index for each stage are indicated. (B) The end of each bar represents the moment of cardioversion. Baseline: 60 min of stabilization period after turning off the pacemaker and preceding the start of the PA-6 infusion; Bolus: administration of 2.5 $mg \cdot kg^{-1}$ PA-6 over 10 min; Maintenance: administration of 0.04 $mg \cdot kg^{-1} \cdot min^{-1}$ PA-6 over the next 50 min; Washout: washout period after the end of PA-6 infusion.

infusion). Compared to baseline, PA-6 prolonged RR and QT times following cardioversion but did not affect QRS duration in AF goats (Table 1).

In two SR goats, PA-6 administration ($2.5\,mg \cdot kg^{-1} \cdot 10\,min^{-1}$) tended to prolong QTc (349 vs 432 ms for goat #1 and 356 vs 376 ms for goat #2) and QRS width (59 vs 71 ms and 59 vs 69 ms) at the end of infusion, but did not consistently affect RR duration (683 vs 542 ms and 665 vs 613 ms).

PA-6 increases AFCL. During PA-6 infusion, the AFCL gradually prolonged, as shown for two goats in Figure 2A, B. The median AFCL was stable during stabilization period in all animals and significantly higher in the LA than in the RA (139 ± 23 vs 111.7 ± 29 ms; $P < 0.05$). The significant difference in AFCL between the atria remained throughout the whole protocol.

The largest increase in AFCL duration occurred during bolus infusion, and this prolongation was significant compared to baseline AFCL for both atria. After infusion of the PA-6 bolus, the AFCL did not show a significant further increase during the maintenance period (Figure 2C). The prolongation of AFCL was somewhat more pronounced in the RA, but the difference in AFCL prolongation between the atria was not significant (Figure 2D).

P5 AFCL values, a surrogate marker for the refractory period, also had significantly lower baseline values in the RA, compared with the LA, and this difference became more pronounced after drug administration (Figure 2E). However, the relative increases in p5 of the AFCL caused by PA-6 were not significantly different between LA and RA (Figure 2F).

PA-6 decreases the complexity of AF

Representative wave maps of three consecutive beats of AF at baseline, during the first minute of maintenance and during the last minute preceding cardioversion are presented in the Figure 3A (left panel). These wave maps show the number of waves, the origin of waves (peripheral or breakthrough) and the size of waves. PA-6 infusion decreased the number of (peripheral and breakthrough) waves, while simultaneously increasing wave size. The right panel of Figure 3A illustrates the concomitant decrease in fractionation index during PA-6 infusion.

The parameters related to AF pattern and complexity confirm that PA-6 decreased AF complexity equally in both atria, by reducing the total number of fibrillation waves and the number of BT waves per AF cycle (Figure 3B, C). This was associated with an increase in wave size (Figure 3D) and a decrease in mean fractionation index (Figure 3E). However, the conduction velocity of fibrillation waves was not affected

Table 1

Electrophysiological parameters (in ms) in AF goats ($n = 5$) that cardioverted during PA-6 application

	Baseline	Bolus (0–1 min)	Pre-conversion (1 min)	Post-conversion (1 min)
RR	310 ± 49	323 ± 40	334 ± 41	583 ± 75*
QRS	41 ± 1	40 ± 3	41 ± 4	40 ± 2
QT	241 ± 33	240 ± 29	257 ± 30	341 ± 34*
QTc	n.d.[a]	n.d.	n.d.	472 ± 29

[a]QTc correction cannot be derived in AF conditions.
*$P < 0.05$ versus baseline.

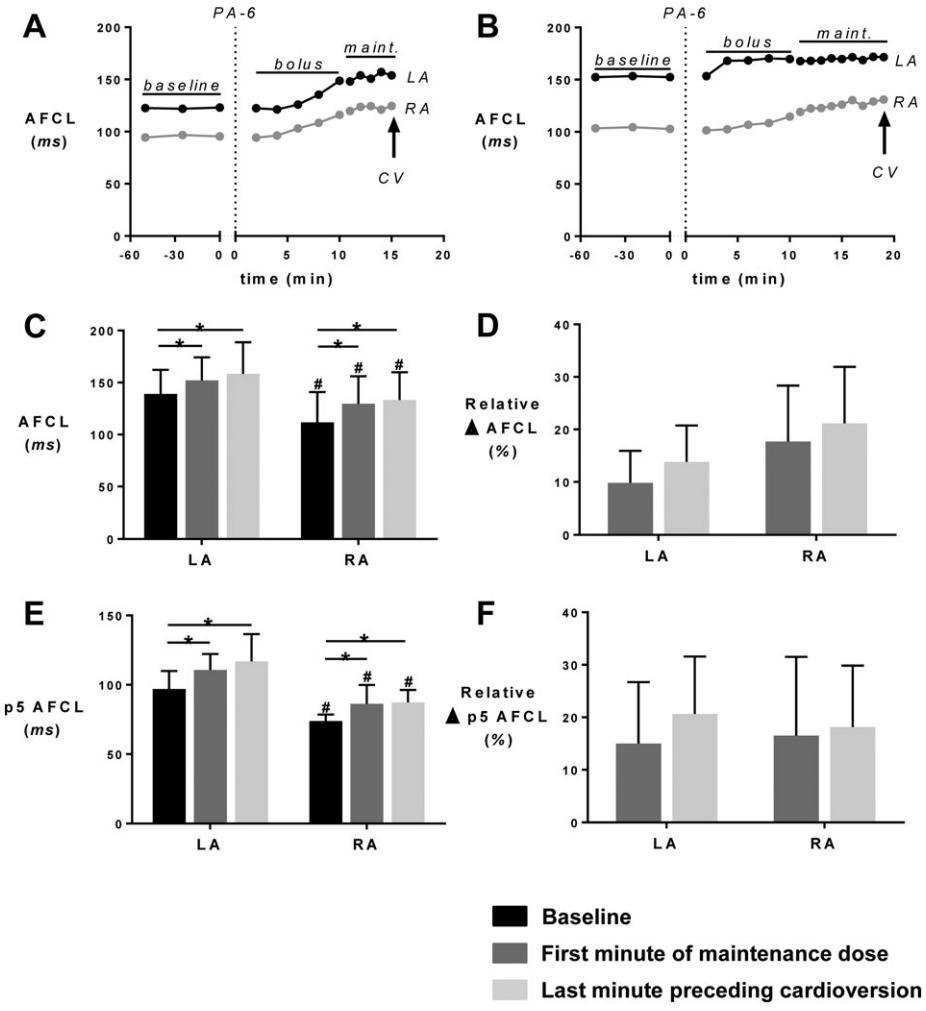

Figure 2

PA-6 lengthens the AFCL. (A, B) Time course for AFCL in both atria during PA-6 infusion until the moment of cardioversion to SR in two goats. CV, cardioversion to SR. (C) AFCL for the LA and RA, (D) relative change in AFCL, (E) p5 of the AFCL and (F) relative change of p5 of the AFCL. All parameters were calculated for the baseline, the first minute of maintenance period (maint. start) and the last minute preceding cardioversion. Data for $n = 5$ goats displaying cardioversion are shown. * $P < 0.05$, significantly different as indicated; #$P<0.05$, significantly different from corresponding value in LA.

by PA-6 (Figure 3F). The decrease in AF complexity was comparable in both atria. A tendency toward organization of AF was present already during the first minute of PA-6 maintenance, and a significant difference compared to baseline values was present during the last minute preceding the cardioversion.

PA-6 lengthens QTc in dogs but does not induce TdP arrhythmias

In SR dogs, PA-6 infused at a dose of either 0.5 or 2.5 $mg{\cdot}kg^{-1}{\cdot}10\ min^{-1}$ did not cause significant effects on RR, PQ, QRS, QTc and LV_{MAPD80} duration or on the pro-arrhythmic marker STV as determined on the LV_{MAP} ($STV_{LVMAPD80}$) (Table 2, Supporting Information Figure S1).

In isolated ventricular cardiomyocytes from cAVB dogs, 200 nM PA-6 inhibited both inward and outward I_{K1} (Figure 4A). In cAVB dogs, PA-6 administration at 2.5 $mg{\cdot}kg^{-1}{\cdot}10\ min^{-1}$ did not significantly alter QRS or STV but prolonged QTc and LV_{MAPD80} durations (Table 2, Supporting Information Figure S2). PA-6 did not induce TdP arrhythmias in nine cAVB dogs (Figure 4B, D). In contrast, the I_{Kr} blocker dofetilide induced TdP arrhythmias in five dogs using the same set of nine animals (Figure 4C, D). Furthermore, dofetilide resulted in more pronounced QTc and LV_{MAPD80} prolongation than PA-6 (Table 2).

PA-6 pharmacokinetics in goats and dogs

Figure 5A provides plasma profile of PA-6 in AF goats. C_{max} (6.7 ± 1.3 μM) was obtained at the end of the bolus. During maintenance infusion, plasma PA-6 concentrations gradually dropped (1.7 ± 0.5 μM). Thirty minutes following the end of maintenance infusion, PA-6 plasma levels were (0.5 ± 0.2 μM). Goat plasma

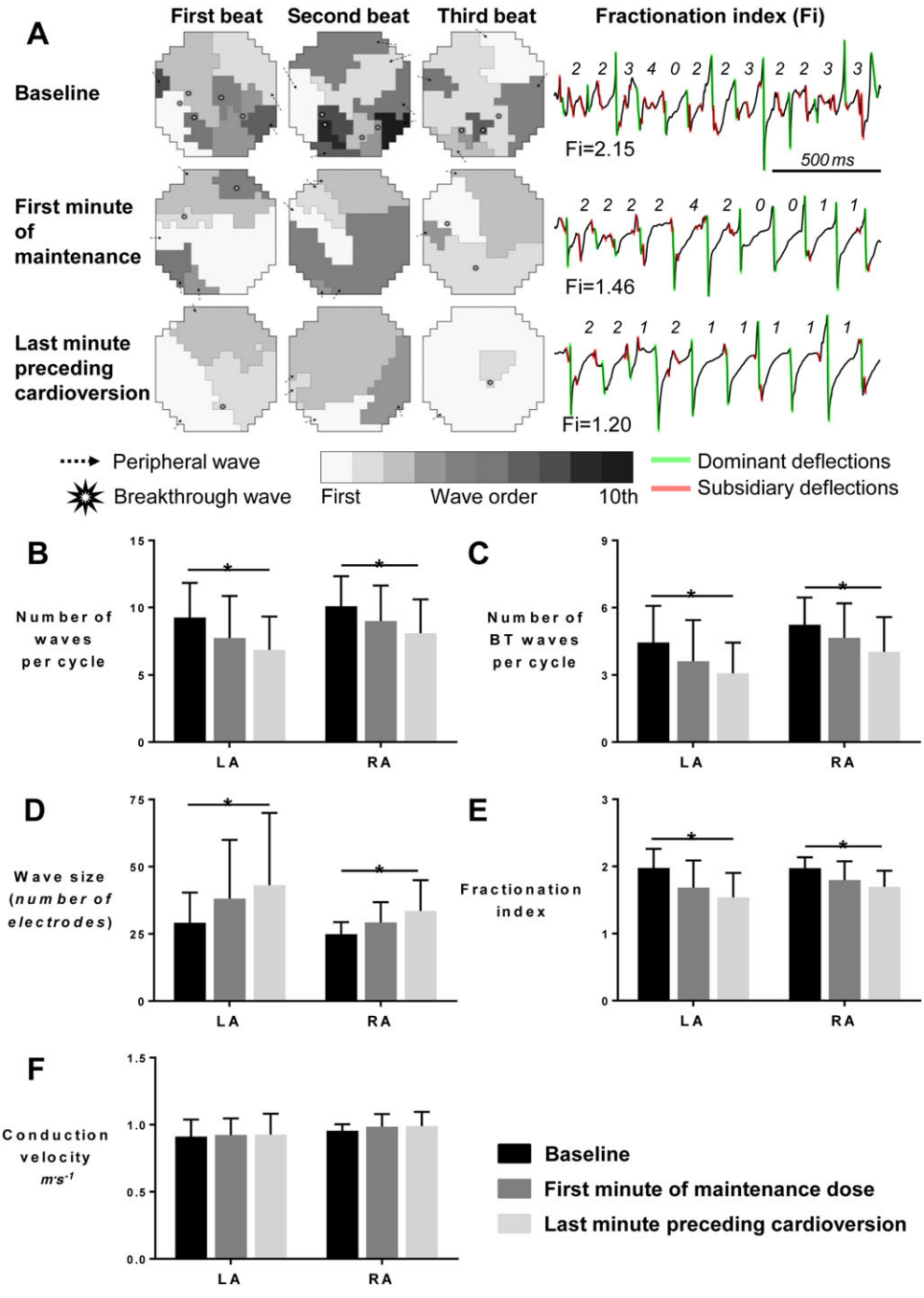

Figure 3

PA-6 decreases the complexity of atrial fibrillation for LA and RA. (A) Fibrillation patterns. Wave maps of three consecutive AF beats at baseline, at the first minute of maintenance and at the last minute preceding cardioversion (left panel) reconstructed based on the mapping data acquired with LA spoon electrode (Ø 4 cm, 247 electrodes, interelectrode distance 2.4 mm). Wave maps depict the total number of waves, origin of the waves (peripheral and breakthrough), wave size and wave order. The right panel depicts the calculation method of the unipolar fractionation indexes at one electrode for three different time points according to dominant activations. The fractionation index is calculated as the ratio between the number of dominant (green) and subsidiary (red) deflections. (B) Total number of waves per cycle, (C) number of epicardial breakthrough waves per cycle, (D) wave size expressed as mean number of electrodes assigned to one wave, (E) fractionation index (mean values of ratios of remote to local deflections per electrode) and (F) mean conduction velocity for each electrode. Data for n = 5 goats displaying cardioversion are depicted in panel B–F. * $P < 0.05$, significantly different as indicated.

Table 2

Electrophysiological parameters (in ms) in sinus rhythm and cAVB dogs in control conditions and upon drug application

	Sinus rhythm (n = 4)		cAVB (n = 9)		cAVB (n = 9)	
	Baseline	PA-6	Baseline	PA-6	Baseline	Dofetilide
RR[a]	601 ± 54	605 ± 55	1000	1000	1000	1000
PQ[b]	129 ± 20	125 ± 18	n.a.	n.a.	n.a.	n.a.
QRS	75 ± 5	75 ± 4	117 ± 9	118 ± 8	115 ± 10	115 ± 11
QTc	306 ± 21	326 ± 16	384 ± 40	465 ± 89*	381 ± 26	600 ± 33*
STV	0.29 ± 0.02	0.39 ± 0.17	0.60 ± 0.22	1.20 ± 0.68	0.77 ± 0.23	1.82 ± 0.88
LV_{MAPD80}	197 ± 21	216 ± 28	236 ± 20	285 ± 52*	249 ± 18	400 ± 64*

[a]cAVB dogs are paced from the right ventricular apex at 1 Hz;
[b]cAVB dog has per definition no PQ conduction;
*$P < 0.05$ versus baseline.

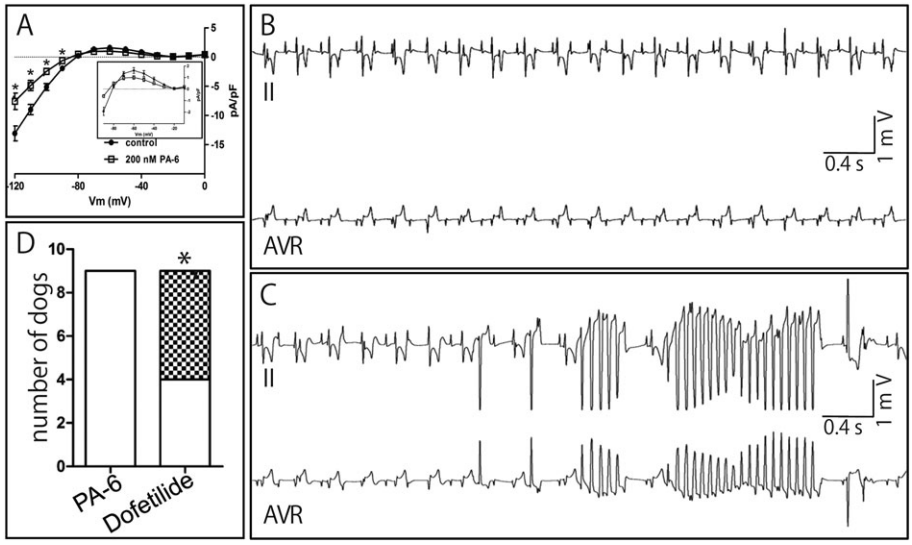

Figure 4

Absence of pro-arrhythmia upon PA-6 application in cAVB dogs. (A) I_{K1} current–voltage relationships from isolated ventricular cAVB cardiomyocytes (n = 8) for control (closed circles) and 200 nM PA-6 (open squares) treatment. Inset: enlargements of currents from −90 to −10 mV. (B) Electrocardiogram (leads II and AVR) displaying normal paced cAVB rhythm following PA-6 (2.5 mg·kg^{-1}·10 min^{-1}) application. (C) Electrocardiogram (leads II and AVR) from the same animal as in panel A, showing TdP arrhythmia episode following dofetilide (25 μg·kg^{-1}·5 min^{-1}) application. (D) Quantification of TdP arrhythmias in nine cAVB animals tested serially with dofetilide and PA-6 (in random order). Non-filled: normal cAVB rhythm; checkered pattern: TdP arrhythmia inducible (three or more TdP arrhythmias). *$P < 0.05$, * $P < 0.05$, significantly different from PA-6.

spiked with PA-6 at 0.5, 1, 5 and 50 μM resulted in a PA-6 unbound fraction of 0.59 ± 0.06% (3.0 nM), 0.67 ± 0.14% (6.7 nM), 1.54 ± 0.35% (77 nM) and 7.41 ± 0.54% (3.7 μM) respectively. During the experiment, skeletal muscle PA-6 levels increased to 3.6 μM. Atrial and ventricular PA-6 concentrations were approximately 8- and 21-fold higher respectively (Table 3).

PA-6 administration to SR (n = 2) and cAVB (n = 2) dogs at the low and high dose resulted in a two-peaked PA-6 plasma profile (Figure 5B). C_{max} at low dose were 0.41 ± 0.18 and 0.47 ± 0.17 μM for SR and cAVB respectively, whereas C_{max} at the high dose were 5.75 ± 1.30 and 5.33 ± 0.63 μM respectively. Thirty minutes following start of administration of the high dose, PA-6 plasma concentration of 0.30 ± 0.12 and 0.44 ± 0.32 μM were achieved for SR and cAVB dogs respectively.

Follow-up QTc measurements in awake cAVB dogs for more than 2 weeks after PA-6 administration at the high dose indicated absence of QTc changes when compared to predosing, either at idioventricular rhythm or when paced from the right ventricle at 1 Hz (Figure 6). Therefore, the

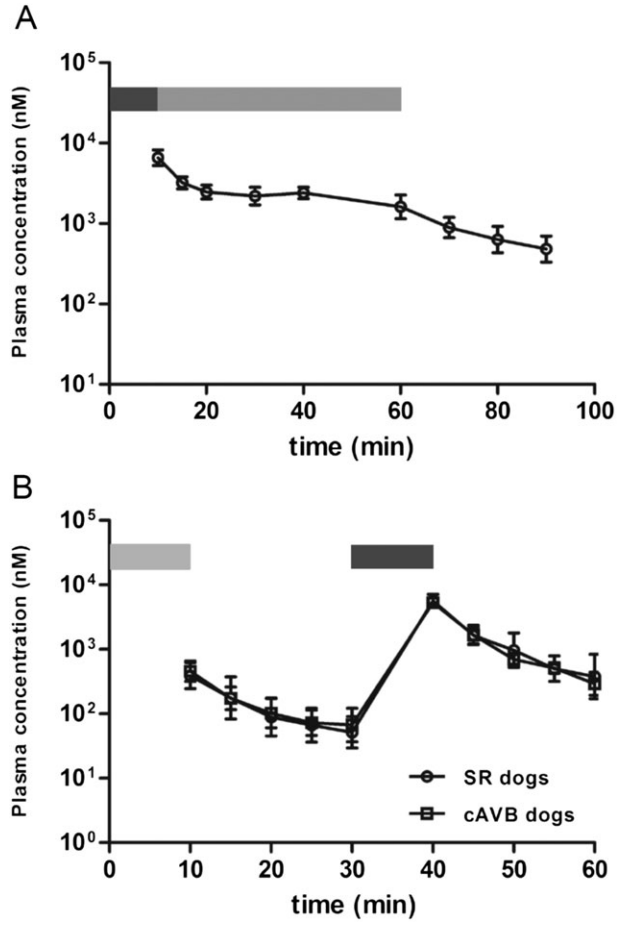

Figure 5

PA-6 plasma concentrations in AF goats and cAVB dogs. (A) PA-6 plasma concentrations (nM) in cardioverted AF goats (n = 5) following PA-6 infusion (0–10 min bolus (2.5 mg·kg^{-1}·10 min^{-1}, dark grey bar), 10–60 min maintenance (0.04 mg·kg^{-1}·min^{-1}, light grey bar), 60–90 min (washout)). (B) PA-6 plasma concentrations in SR (n = 2) and cAVB dogs (n = 2) following a low dose [0–10 min (0.5 mg·kg^{-1}·10 min^{-1}, light grey bar)] and a high dose (30–40 min 2.5 mg·kg^{-1}·10 min^{-1}, dark grey bar) bolus. Washout between 10–30 and 40–60 min respectively.

Table 3

PA-6 tissue concentrations (μM) after start of infusion

Tissue	10 min	20 min	60 min
Skeletal Muscle	2.3 ± 2	2.6 ± 1	3.6 ± 2
Right ventricle	n.a.	n.a.	78 ± 14
Left ventricle	n.a.	n.a.	70 ± 21
Right atrium	n.a.	n.a.	29 ± 4
Left atrium	n.a.	n.a.	30 ± 6

observed QTc prolongation during the experiment (t = 30 min) (Table 2, Supporting Information Figure S2) was not persistent during follow-up, suggesting rapid clearance from cardiac tissue.

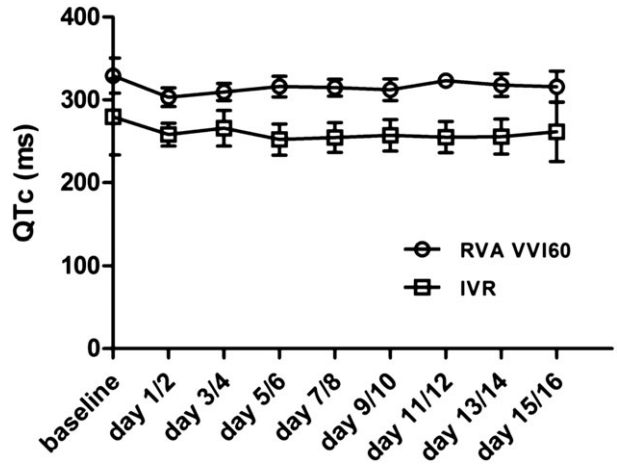

Figure 6

Absence of chronic QTc interval prolongation in cAVB dogs (n = 9) upon 16 days post-infusion. ECG recordings were taken in awake animals during idioventricular rhythm (IVR) or right ventricular apex pacing at 1 Hz (RVA VVI60).

PA-6 inhibits basal I_{K1} in human atrial cardiomyocytes

Typical current traces and current amplitudes at −100 mV in the time course of an experiment are shown in Figure 7A, B. Cell capacitances averaged 107.0 ± 7.2 pF (n = 26). Agonist-independent basal current was measured by applying a depolarizing ramp pulse from −100 to +40 mV [holding potential −80 mV; 112 (mV/s); see inset in Figure 7A, C]. Ba^{2+} (1 mM) was applied at the end of each experiments in each cardiomyocyte, and the inward rectifier K^+ currents were analysed after subtraction of the resulting leak currents.

Application of 2 μM **carbachol** (CCh) resulted in rapid initial increase ('Peak') of $I_{K,ACh}$ amplitude followed by a decrease to a 'quasi steady-state' level despite continuous presence of CCh ('desensitization') (Dobrev *et al.*, 2005; Figure 7B). $I_{K,ACh}$ was defined as the CCh-sensitive current increase (Dobrev *et al.*, 2005; Voigt *et al.*, 2007). PA-6 (200 nM) was applied after 1 min washout of CCh and resulted in an immediate and maintained block of I_{K1} (Figure 7B, D). CCh (2 μM) was applied a second time with the first (S1) application serving as internal control, the second (S2) being measured in the presence of PA-6 (Figure 7A). $I_{K,ACh}$ was smaller during S2 than S1 suggesting incomplete recovery from desensitization, but the degrees of $I_{K,ACh}$ desensitization, expressed as S2/S1 ratio, were similar in PA-6 experiments and in time-matched controls (Figure 7B, E).

Discussion

Here, we demonstrated, by using two established large animal models for efficacy and safety testing, the validity of I_{K1} as a safe drug target in AF therapy. We showed that the specific I_{K1} inhibitor PA-6 is indeed able to inhibit AF in a goat model of pacing induced AF. Our results demonstrate that

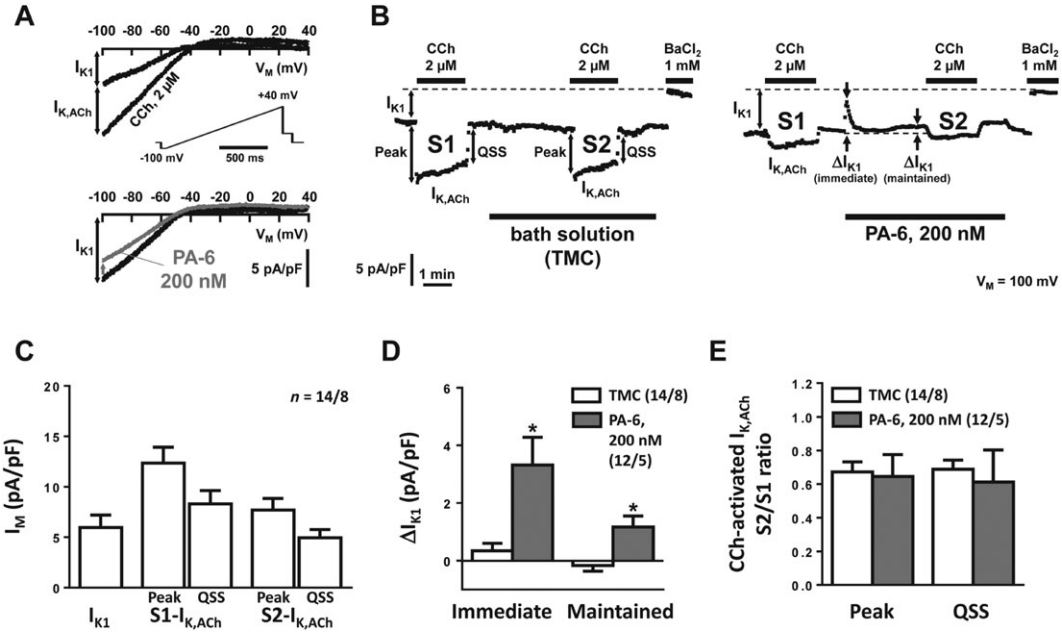

Figure 7

Effect of PA-6 (200 nM) on inward rectifier K^+ currents in human atrial cardiomyocytes. (A) Original recording of basal current with response to 2 μM carbachol (CCh; upper panel; $I_{K,ACh}$ was defined as CCh-sensitive current) and response to 200 nM PA-6 (lower panel). (B) Time course of I_{K1} and $I_{K,ACh}$ during two successive CCh applications (S1, S2, 4 min apart). During activation the initial increase ('Peak') of $I_{K,ACh}$ faded ('rapid desensitization') to a quasi-steady-state level ('QSS'). PA-6 (200 nM) was applied 1 min after the first CCh application (right panel) and compared with application of bath solution only (left panel; time-matched controls, TMC). (C) Basal current and CCh-activated $I_{K,ACh}$ at 'Peak' and 'QSS'. (D, E) Effects of PA-6 (200 nM) on basal current and on the S2/S1 ratio of $I_{K,ACh}$ at 'Peak' and 'QSS'. Data are expressed as mean ± SEM. *$P < 0.05$, * $P < 0.05$, significantly different from time-matched controls (TMC). Numbers indicate cardiomyocytes/patients.

cardioversion is preceded by prolongation of AF cycle length and an increase in atrial refractoriness and a concomitant decrease in AF complexity. The conduction velocity of atrial fibrillation waves was not affected.

Among the many changes that occur during AF progression, increases in $K_{ir}2.1$ function, protein and mRNA expression were found in several studies comparing AF patients of different aetiology with matched controls (Veldhuis *et al.,* 2015). For this reason, pharmacological inhibition of I_{K1} was suggested as a new treatment option (Ehrlich, 2008; Bhave *et al.,* 2010), although the potential side effects of neurological, ventricular-, skeletal- and smooth-muscle related complications may have hampered development of specific I_{K1} inhibiting compounds for this purpose.

In Langendorff-perfused sheep heart, chloroquine, which inhibits I_{K1} (IC_{50} = 0.69 μM), I_{KACh} (IC_{50} = 0.38 μM) and I_{KATP} (IC_{50} = 0.51 μM) channels, terminated stretch-induced AF at concentrations between 1 and 4 μM (Filgueiras-Rama *et al.,* 2012) and cholinergically induced AF at 10 μM (Noujaim *et al.,* 2011). The authors reported that chloroquine decreased AF frequency and the number of breakthrough waves just before AF termination, as we found in our *in vivo* PA-6 experiments in goats. We show that PA-6 increases the AFCL and AERP (as shown by the surrogate parameter of the p5 of the AFCL histogram) (Duytschaever *et al.,* 2001). The decrease in the total number of waves and breakthrough waves per AF cycle and an increase in the size of fibrillation waves indicate that PA-6 makes the fibrillation pattern much simpler. Previously, we showed that progressive atrial electrical and structural remodelling make the fibrillation pattern more complex and thereby make AF more stable (Eckstein *et al.,* 2011; Verheule *et al.,* 2010, 2014). Conversely, a decrease in AF complexity, as observed during PA-6 infusion, would make AF less stable and therefore AF termination more likely.

I_{K1} may have a pivotal role in rotor stability (Beaumont *et al.,* 1998; Noujaim *et al.,* 2007), and we would expect that PA-6 impairs rotor stability. We have not observed stable rotors in the mapped atrial regions. However, rotors may have been present outside our field of view, such as the posterior LA, which in the goat is not accessible for epicardial mapping. Nevertheless, our results are fully compatible with a decrease in rotor stability with I_{K1} blockade. With decreased rotor stability and frequency, break-up into 'daughter waves' (Everett and Olgin, 2004), and therefore, the complexity of fibrillatory patterns at more distant sites would also be reduced. Therefore, irrespective of the mechanism responsible for AF maintenance, multiple wavelets or rotors with 'daughter waves', the decrease in AF complexity would be related to a decrease in AF stability.

Class IC and III anti-arrhythmic drugs were evaluated earlier in the same goat model used here. In general, Class IC blockers primarily cause a reduction in conduction velocity, whereas class III inhibitors increase AERP, but all

drugs that can successfully terminate AF reduce the complexity of AF, regardless of the observed prolongation in AFCL. Following 3 to 4 weeks of pacing induced persistent AF, cibenzoline resulted in cardioversion rates of 78% (Eijsbouts *et al.,* 2006), flecainide in 33 and 67% (Wijffels *et al.,* 1999; Eijsbouts *et al.,* 2006), d-Sotalol in 92% (Wijffels *et al.,* 1999) and the combination of AVE0118 + dofetilide in 100% (Blaauw *et al.,* 2007). PA-6 administration, at similar times following AF induction, resulted in a cardioversion rate of 83% and thereby performs better than flecainide, comparable to cibenzoline and combined AVE0118 +- dofetilide application, but less efficient than d-sotalol. Direct comparison of these drugs, even in the same animal model, is not straightforward, because of the different dosages used. However, all studies used up to the highest tolerated dose and had similar safety endpoints with respect to QRS duration and ventricular proarrhythmia. Importantly, the efficacy of cardioversion of a particular drug can be species-specific. For example, although d-sotalol was highly successful in restoring SR in goats, it was less effective than flecainide in humans and therefore is not used in clinical practice for pharmacological cardioversions (Reisinger *et al.,* 1998; Kirchhof *et al.,* 2016).

The present study reflect an early point in the development of AF-induced remodelling. A decrease of cardioversion rate upon AF progression in the AF goat model, measured in awake goats, was observed for flecainide (60, 33, 33 and 17% at 1, 4, 8 and 16 weeks of AF respectively), cibenzoline (80, 78, 67 and 63% at 1, 4, 8 and 16 weeks of AF respectively) (Eijsbouts *et al.,* 2006) and AVE0118 + dofetilide (80, 33, 50, 0, 0 and 0% at 1, 2, 3, 4, 5 and 6 months of AF respectively) (Verheule *et al.,* 2010). Follow-up studies with PA-6 are required to determine efficacy at later time points during AF-induced remodelling.

We used the cAVB dog to investigate the potential pro-arrhythmic actions of PA-6. Previously, we used this model to investigate the pro-arrhythmic and anti-arrhythmic actions of various clinically used drugs and experimental compounds, including anti-AF drugs (Thomsen *et al.,* 2006; Oros *et al.,* 2008; Antoons *et al.,* 2010; Bourgonje *et al.,* 2013; Varkevisser *et al.,* 2013). This is the first study that investigates specific I_{K1} inhibition in this model. In SR animals, no reduction in conduction velocity was evidenced by either PQ or QRS interval changes, whereas QTc prolongation was less than 7%. The cAVB dog, with its compromised repolarization reserve (Oros *et al.,* 2008), showed a more severe QTc prolongation (21%), whereas also here ventricular activation (QRS width) was not impaired. Moreover, no pro-arrhythmia was observed in contrast to dofetilide application in the serially tested animals. I_{K1} inhibition was proposed to be pro-arrhythmic (Escande *et al.,* 1986). This view is mainly based on experiments in which $BaCl_2$ was applied to small and large animal models. As argued by us earlier, specific inhibition of I_{K1} by $BaCl_2$ is not pro-arrhythmic and has only minor effects on the resting membrane potential in various animal models and isolated tissues (Van der Heyden and Jespersen, 2016). Only at higher concentrations of $BaCl_2$ (>10 μM), when $I_{K,Ach}$ and $I_{K,ATP}$ channels become affected also, resting membrane depolarization and arrhythmic events become evident. In classical experiments performed by Roza and Berman (1971), infusion of 1 $\mu mol \cdot kg^{-1} \cdot min^{-1}$ of $BaCl_2$ in normal dogs under anaesthesia resulted in a course of events that eventually resulted in hypotension, flaccid paralysis of skeletal muscles, ventricular tachycardia and fibrillation (Roza and Berman, 1971). Finally, hypokalaemia occurred, most likely resulting from an extra-intracellular potassium shift. This findings strongly reflects the course seen in barium poisoning cases in man (Bhoelan *et al.,* 2014). Interestingly, potassium administration to dogs counteracted most of the clinical signs (Roza and Berman, 1971). No serum potassium levels were measured in our canine experiments, although we expect these to be already low, as earlier studies demonstrated serum potassium concentrations of 2.8 mM in the experimental setting of the cAVB dogs (Thomsen *et al.,* 2006).

It cannot be excluded that the effects of PA-6 are species dependent, but when we compare PA-6-mediated block between human and white bream (fish) $K_{ir}2.1$, that share 82.9% sequence identity at the protein level, no differences in blockade were obtained (Supporting Information Figure S3). Amino acid sequence identities for $K_{ir}2.1$, $K_{ir}2.2$ and $K_{ir}2.3$ between human, dog and goat are significantly higher (95–99%) (Supporting Information Figure S4). As demonstrated before, $K_{ir}2.1$, $K_{ir}2.2$ and $K_{ir}2.3$ channels have similar sensitivities to PA-6 (Takanari *et al.,* 2013). For these reasons, we do not anticipate that channel differences due to isoform expression alterations or sequence variation between species would affect outcome. However, species-dependent differences in I_{K1} density may have an effect on pro- and anti-arrhythmic effects. In a direct comparison, ventricular I_{K1} density in canine ventricular cells is twofold to threefold higher than in human ventricular cardiomyocytes (Jost *et al.,* 2013) which may increase the sensitivity of the human ventricle for I_{K1} inhibition compared to dog. Furthermore, I_{K1} densities found in the atrium are 10-fold (Cordeiro *et al.,* 2015) or fivefold (Wang *et al.,* 1998) lower than in the ventricle of dogs and humans respectively, which may provide a safety margin for anti-arrhythmic I_{K1} inhibition in the atrium and pro-arrhythmic activity in the ventricle. Finally, we provided evidence that also human atrial I_{K1} is a target for PA-6. For the goat, $K_{ir}2.x$ isoform expression data and accompanying I_{K1} densities are currently not available and deserve further attention.

Recently, the effects of PA-6 application to Langendorff-perfused rat hearts were reported (Skarsfeldt *et al.,* 2016). In contrast to our findings, no lengthening of the atrial ERP was observed. The authors observed prolongation of the ventricular AP and ventricular fibrillation occurred in two out of six hearts assessed. Several factors may explain the differences between our findings and those of Skarsfeldt *et al.* (2016). The relative contribution of I_{K1} to atrial and ventricular repolarization and resting membrane potential stability is likely to differ between murine and many other animal models, as well as its blockade by PA-6 may result in different pro-arrhythmic liability, as brought forward in the Skarsfeldt report (Skarsfeldt *et al.,* 2016). Interestingly, a recent paper involving the same research group on Langendorff-perfused guinea pig hearts did not report any

pro-arrhythmia of PA-6 (Hoeker *et al.,* 2017). The authors emphasized that the relative contribution of I_{K1} to repolarization is lower in guinea pig than in rat. Secondly, our *in vivo* models include factors like autonomic regulation, mechanical function and anaesthesia, which all affect cardiac function differently, whereas an *ex vivo* Langendorff heart model lacks these factors.

The lipophilic PA-6 accumulates in cardiac tissues as established here, especially in the ventricle. Currently, we cannot provide a clear explanation for this phenomenon. It is however tempting to speculate that the high levels of expression of I_{K1} channels, especially in the canine ventricle (Cordeiro *et al.,* 2015), may be the basis of this finding.

Our current results, obtained from goats and dogs, demonstrates cardiac safety and good anti-AF properties for PA-6. Furthermore, PA-6 is able to target human atrial I_{K1}. Therefore, PA-6 might be considered as an interesting compound for further clinical evaluation as a potential anti-arrhythmic drug for AF.

Limitations

An important limitation of our study is that cardioversion efficacy of PA-6 in the goat model of AF was tested in animals under general anaesthesia. The anaesthesia regimen contained thiopental which is a known I_{K1} inhibitor that most likely acts *via* interfering with PIP_2 (Van der Heyden *et al.,* 2013). Furthermore, conversion was tested at 3 weeks of pacing-induced AF only. Given the current study set-up, we cannot exclude that potential PA-6 activity outside the heart contributes to the anti-arrhythmic efficacy nor can we exclude that additional potassium currents within the goat atrium are involved.

Current safety studies focused on cardiac arrhythmias in the cAVB dog only. At this point, no statements can be made on skeletal muscle, including respiratory muscle, and neurological effects and these questions await further analysis. This study made use of a single-dose regimen for efficacy and safety testing in large animal studies. A full dose–response relationship, both with respect to efficacy and toxicity, should be performed prior to considering any human clinical testing.

Acknowledgements

The authors thank Monika Hagedorn for excellent technical assistance.

Y.J. is the recipient of a scholarship from the Chinese Scholarship Council. This study received funding from the UMC Utrecht holding b.v. (Octopus valorization grant). D.D. is supported by the National Institutes of Health (R01-HL131517), the German Research Foundation DFG (Do 769/4-1) and DZHK (German Center for Cardiovascular Research). N.V. is supported by the DZHK, by the German Research Foundation (DFG VO 1568/3-1 and IRTG1816 RP12) and by the Else-Kröner-Fresenius Stiftung (EKFS 2016_A20). S.V. is supported by the European Union; EUTRAF (No. 261057) and the Dutch Heart Foundation; RACE-V (CVON201409). D.O. is supported by a scholarship from the Serbian Ministry of Youth and Sports; Fund for Young Talents – Dositeja. S.V. and D.O are both supported by RADOX (No. 316738).

Author contributions

Y.J., R.V., D.O., A.B., A.P.K. and M.Z. planned and performed the experiments and analysed the data. M.K. and J.D.M.B. performed the experiments and the analysed data. M.Z.W., S.V., D.D., N.V., M.V. and M.A.G.v.d.H. designed the study, planned the experiments and analysed data. Y.J., S.V., M.Z. W., N.V. and M.A.G.v.d.H wrote the manuscript.

Conflict of interest

The authors declare no conflicts of interest.

Declaration of transparency and scientific rigour

This Declaration acknowledges that this paper adheres to the principles for transparent reporting and scientific rigour of preclinical research recommended by funding agencies, publishers and other organisations engaged with supporting research.

References

Alexander SPH, Catterall WA, Kelly E, Marrion N, Peters JA, Benson HE *et al*. (2015). The Concise Guide to PHARMACOLOGY 2015/16: Voltage-gated ion channels. Br J Pharmacol 172: 5904–5941.

Antoons G, Oros A, Beekman JD, Engelen MA, Houtman MJ, Belardinelli L *et al*. (2010). Late Na^+ current inhibition by ranolazine reduces torsades de pointes in the chronic atrioventricular block dog model. J Am Coll Cardiol 55: 801–809.

Beaumont J, Davidenko N, Davidenko JM, Jalife J (1998). Spiral waves in two-dimensional models of ventricular muscle: formation of a stationary core. Biophys J 75: 1–14.

Benjamin EJ, Wolf PA, D'Agostino RB, Silbershatz H, Kannel WB, Levy D (1998). Impact of atrial fibrillation on the risk of death: the Framingham Heart Study. Circulation 98: 946–952.

Bhave G, Lonergan D, Chauder BA, Denton JS (2010). Small-molecule modulators of inward rectifier K^+ channels: recent advances and future possibilities. Future Med Chem 2: 757–774.

Bhoelan BS, Stevering CH, van der Boog AT, Van der Heyden MAG (2014). Barium toxicity and the role of the potassium inward rectifier current. Clin Toxicol (Phila) 52: 584–593.

Biliczki P, Virág L, Iost N, Papp JG, Varró A (2002). Interaction of different potassium channels in cardiac repolarization in dog ventricular preparations: role of repolarization reserve. Br J Pharmacol 137: 361–368.

Blaauw Y, Schotten U, van Hunnik A, Neuberger HR, Allessie MA (2007). Cardioversion of persistent atrial fibrillation by a combination of atrial specific and non-specific class III drugs in the goat. Cardiovasc Res 75: 89–98.

Bosch RF, Zeng X, Grammer JB, Popovic K, Mewis C, Kühlkamp V (1999). Ionic mechanisms of electrical remodeling in human atrial fibrillation. Cardiovasc Res 44: 121–131.

Bourgonje VJ, Vos MA, Ozdemir S, Doisne N, Acsai K, Varro A *et al.* (2013). Combined Na^+/Ca^{2+} exchanger and L-type calcium channel block as a potential strategy to suppress arrhythmias and maintain ventricular function. Circ Arrhythm Electrophysiol 6: 371–379.

Camm AJ, Kirchhof P, Lip GY, Schotten U, Savelieva I, Ernst S *et al.* (2010). Guidelines for the management of atrial fibrillation: the Task Force for the Management of Atrial Fibrillation of the European Society of Cardiology (ESC). Eur Heart J 31: 2369–2429.

Camm AJ, Lip GY, De Caterina R, Savelieva I, Atar D, Hohnloser SH *et al.* (2012). 2012 focused update of the ESC Guidelines for the management of atrial fibrillation: an update of the 2010 ESC Guidelines for the management of atrial fibrillation. Developed with the special contribution of the European Heart Rhythm Association. Eur Heart J 33: 2719–2747.

Chinitz JS, Halperin JL, Reddy VY, Fuster V (2012). Rate or rhythm control for atrial fibrillation: update and controversies. Am J Med 125: 1049–1056.

Cordeiro JM, Zeina T, Goodrow R, Kaplan AD, Thomas LM, Nesterenko VV*et al.* (2015). Regional variation of the inwardly rectifying potassium current in the canine heart and the contributions to differences in action potential repolarization. J Mol Cell Cardiol 84: 52–60.

Curtis MJ, Bond RA, Spina D, Ahluwalia A, Alexander SP, Giembycz MA *et al.* (2015). Experimental design and analysis and their reporting: new guidance for publication in BJP. Br J Pharmacol 172: 3461–3471.

De Boer TP, Houtman MJ, Compier M, van der Heyden MAG (2010a). The mammalian $K_{IR}2.x$ inward rectifier ion channel family: expression pattern and pathophysiology. Acta Physiol (Oxf) 199: 243–256.

De Boer TP, Nalos L, Stary A, Kok B, Houtman MJ, Antoons G *et al.* (2010b). The anti-protozoal drug pentamidine blocks $K_{IR}2.x$-mediated inward rectifier current by entering the cytoplasmic pore region of the channel. Br J Pharmacol 159: 1532–1541.

Dobrev D, Friedrich A, Voigt N, Jost N, Wettwer E, Christ T*et al.* (2005). The G protein-gated potassium current $I_{K,ACh}$ is constitutively active in patients with chronic atrial fibrillation. Circulation 112: 3697–3706.

Dobrev D, Graf E, Wettwer E, Himmel HM, Hála O, Doerfel C *et al.* (2001). Molecular basis of downregulation of G-protein-coupled inward rectifying K^+ current ($I_{K,ACh}$) in chronic human atrial fibrillation: decrease in GIRK4 mRNA correlates with reduced $I_{K,ACh}$ and muscarinic receptor-mediated shortening of action potentials. Circulation 104: 2551–2557.

Dobrev D, Wettwer E, Kortner A, Knaut M, Schüler S, Ravens U (2002). Human inward rectifier potassium channels in chronic and postoperative atrial fibrillation. Cardiovasc Res 54: 397–404.

Duytschaever M, Mast F, Killian M, Blaauw Y, Wijffels M, Allessie M (2001). Methods for determining the refractory period and excitable gap during persistent atrial fibrillation in the goat. Circulation 104: 957–962.

Eckstein J, Maesen B, Linz D, Zeemering S, van Hunnik A, Verheule S *et al.* (2011). Time course and mechanisms of endo-epicardial electrical dissociation during atrial fibrillation in the goat. Cardiovasc Res 89: 816–824.

Eckstein J, Zeemering S, Linz D, Maesen B, Verheule S, van Hunnik A *et al.* (2013). Transmural conduction is the predominant mechanism of breakthrough during atrial fibrillation: evidence from simultaneous endo-epicardial high-density activation mapping. Circ Arrhythm Electrophysiol 6: 334–341.

Ehrlich JR (2008). Inward rectifier potassium currents as a target for atrial fibrillation therapy. J Cardiovasc Pharmacol 52: 129–135.

Eijsbouts S, Ausma J, Blaauw Y, Schotten U, Duytschaever M, Allessie MA (2006). Serial cardioversion by class IC drugs during 4 months of persistent atrial fibrillation in the goat. J Cardiovasc Electrophysiol 17: 648–654.

Escande D, Coraboeuf E, Planché C, Lacour-Gayet F (1986). Effects of potassium conductance inhibitors on spontaneous diastolic depolarization and abnormal automaticity in human atrial fibers. Basic Res Cardiol 81: 244–257.

Everett TH 4th, Olgin JE (2004). Basic mechanisms of atrial fibrillation. Cardiol Clin 22: 9–20.

Filgueiras-Rama D, Martins RP, Mironov S, Yamazaki M, Calvo CJ, Ennis SR *et al.* (2012). Chloroquine terminates stretch-induced atrial fibrillation more effectively than flecainide in the sheep heart. Circ Arrhythm Electrophysiol 5: 561–570.

Gillis AM, Krahn AD, Skanes AC, Nattel S (2013). Management of atrial fibrillation in the year 2033: new concepts, tools, and applications leading to personalized medicine. Can J Cardiol 29: 1141–1146.

Heijman J, Voigt N, Nattel S, Dobrev D (2014). Cellular and molecular electrophysiology of atrial fibrillation initiation, maintenance, and progression. Circ Res 114: 1483–1499.

Hibino H, Inanobe A, Furutani K, Murakami S, Findlay I, Kurachi Y (2010). Inwardly rectifying potassium channels: their structure, function, and physiological roles. Physiol Rev 90: 291–366.

Hoeker GS, Skarsfeldt MA, Jespersen T, Poelzing S (2017). Electrophysiologic effects of the I_{K1} inhibitor PA-6 are modulated by extracellular potassium in isolated guinea pig hearts. Physiol Rep 5: e13120.

Jost N, Virág L, Comtois P, Ordög B, Szuts V, Seprényi G *et al.* (2013). Ionic mechanisms limiting cardiac repolarization reserve in humans compared to dogs. J Physiol 591: 4189–4206.

Kilkenny C, Browne W, Cuthill IC, Emerson M, Altman DG (2010). Animal research: reporting in vivo experiments: the ARRIVE guidelines. Br J Pharmacol 160: 1577–1579.

Kirchhof P, Benussi S, Kotecha D, Ahlsson A, Atar D, Casadei B *et al.* (2016). 2016 ESC Guidelines for the management of atrial fibrillation developed in collaboration with EACTS. Eur Heart J 37: 2893–2962.

Krahn AD, Manfreda J, Tate RB, Mathewson FA, Cuddy TE (1995). The natural history of atrial fibrillation: incidence, risk factors, and prognosis in the Manitoba follow-up study. Am J Med 98: 476–484.

Krijthe BP, Kunst A, Benjamin EJ, Lip GY, Franco OH, Hofman A *et al.* (2013). Projections on the number of individuals with atrial fibrillation in the European Union, from 2000 to 2060. Eur Heart J 34: 2746–2751.

Lau DH, Maesen B, Zeemering S, Kuklik P, van Hunnik A, Lankveld TA *et al.* (2015). Indices of bipolar complex fractionated atrial electrograms correlate poorly with each other and atrial fibrillation substrate complexity. Heart Rhythm 12: 1415–1423.

McGrath JC, Lilley E (2015). Implementing guidelines on reporting research using animals (ARRIVE etc.): new requirements for publication in BJP. Br J Pharmacol 172: 3189–3193.

Mohan NK, Niyogi D, Singh HN (2009). Analysis of relationship between Q-T and R-R interval in the electrocardiogram of goats. Indian J Anim Sci 79: 362–365.

Nagy N, Acsai K, Kormos A, Sebők Z, Farkas AS, Jost N *et al.* (2013). $[Ca^{2+}]_i$-induced augmentation of the inward rectifier potassium current (I_{K1}) in canine and human ventricular myocardium. Pflugers Arch 465: 1621–1635.

Nalos L, Varkevisser R, Jonsson MK, Houtman MJ, Beekman JD, van der Nagel R *et al.* (2012). Comparison of the I_{Kr} blockers moxifloxacin, dofetilide and E-4031 in five screening models of pro-arrhythmia reveals lack of specificity of isolated cardiomyocytes. Br J Pharmacol 165: 467–478.

Noujaim SF, Pandit SV, Berenfeld O, Vikstrom K, Cerrone M, Mironov S *et al.* (2007). Up-regulation of the inward rectifier K^+ current (I_{K1}) in the mouse heart accelerates and stabilizes rotors. J Physiol 578: 315–326.

Noujaim SF, Stuckey JA, Ponce-Balbuena D, Ferrer-Villada T, López-Izquierdo A, Pandit SV*et al.* (2011). Structural bases for the different anti-fibrillatory effects of chloroquine and quinidine. Cardiovasc Res 89: 862–869.

Oros A, Beekman JD, Vos MA (2008). The canine model with chronic, complete atrio-ventricular block. Pharmacol Ther 119: 168–178.

Potpara TS, Stankovic GR, Beleslin BD, Polovina MM, Marinkovic JM, Ostojic MC *et al.* (2012). A 12-year follow-up study of patients with newly diagnosed lone atrial fibrillation: implications of arrhythmia progression on prognosis: the Belgrade Atrial Fibrillation study. Chest 141: 339–347.

Reisinger J, Gatterer E, Heinze G, Wiesinger K, Zeindlhofer E, Gattermeier M *et al.* (1998). Prospective comparison of flecainide versus sotalol for immediate cardioversion of atrial fibrillation. Am J Cardiol 81: 1450–1454.

Roza O, Berman LB (1971). The pathophysiology of barium: hypokalemic and cardiovascular effects. J Pharmacol Exp Ther 177: 433–439.

Satoh HJ (2003). Sino-atrial nodal cells of mammalian hearts: ionic currents and gene expression of pacemaker ionic channels. J Smooth Muscle Res 39: 175–193.

Schotten U, Verheule S, Kirchhof P, Goette A (2011). Pathophysiological mechanisms of atrial fibrillation: a translational appraisal. Physiol Rev 91: 265–325.

Skarsfeldt MA, Carstensen H, Skibsbye L, Tang C, Buhl R, Bentzen BH *et al.* (2016). Pharmacological inhibition of I_{K1} by PA-6 in isolated rat hearts affects ventricular repolarization and refractoriness. Physiol Rep 4: e12734.

Southan C, Sharman JL, Benson HE, Faccenda E, Pawson AJ, Alexander SP *et al.* (2016). The IUPHAR/BPS Guide to PHARMACOLOGY in 2016: towards curated quantitative interactions between 1300 protein targets and 6000 ligands. Nucl Acids Res 44: D1054–D1068.

Takanari H, Nalos L, Stary-Weinzinger A, De Git KC, Varkevisser R, Linder T*et al.* (2013). Efficient and specific cardiac I_{K1} inhibition by a new pentamidine analogue. Cardiovasc Res 99: 203–214.

Thomsen MB, Volders PG, Beekman JD, Matz J, Vos MA (2006). Beat-to-Beat variability of repolarization determines proarrhythmic outcome in dogs susceptible to drug-induced torsades de pointes. J Am Coll Cardiol 48: 1268–1276.

Van der Heyden MAG, Jespersen T (2016). Pharmacological exploration of the resting membrane potential reserve. Impact on atrial fibrillation. Eur J Pharmacol 771: 56–64.

Van der Heyden MAG, Stary-Weinzinger A, Sanchez-Chapula JA (2013). Inhibition of cardiac inward rectifier currents by cationic amphiphilic drugs. Curr Mol Med 13: 1284–1298.

Varkevisser R, van der Heyden MAG, Tieland RG, Beekman JD, Vos MA (2013). Vernakalant is devoid of proarrhythmic effects in the complete AV block dog model. Eur J Pharmacol 720: 49–54.

Veldhuis MG, Ji Y, Van der Heyden MAG (2015). A little too much: cardiac electrophysiological effects of elevated inward rectifying current carried by the $K_{IR}2.1$ ion channel protein. Adapt Med 7: 1–8.

Verheule S, Eckstein J, Linz D, Maesen B, Bidar E, Gharaviri A *et al.* (2014). Role of endo-epicardial dissociation of electrical activity and transmural conduction in the development of persistent atrial fibrillation. Prog Biophys Mol Biol 115: 173–185.

Verheule S, Tuyls E, Gharaviri A, Hulsmans S, van Hunnik A, Kuiper M *et al.* (2013). Loss of continuity in the thin epicardial layer because of endomysial fibrosis increases the complexity of atrial fibrillatory conduction. Circ Arrhythm Electrophysiol 6: 202–211.

Verheule S, Tuyls E, van Hunnik A, Kuiper M, Schotten U, Allessie M (2010). Fibrillatory conduction in the atrial free walls of goats in persistent and permanent atrial fibrillation. Circ Arrhythm Electrophysiol 3: 590–599.

Voigt N, Friedrich A, Bock M, Wettwer E, Christ T, Knaut M *et al.* (2007). Differential phosphorylation-dependent regulation of constitutively active and muscarinic receptor-activated $I_{K,ACh}$ channels in patients with chronic atrial fibrillation. Cardiovasc Res 74: 426–437.

Voigt N, Pearman CM, Dobrev D, Dibb KM (2015). Methods for isolating atrial cells from large mammals and humans. J Mol Cell Cardiol 86: 187–198.

Voigt N, Trausch A, Knaut M, Matschke K, Varro A, Van Wagoner DR *et al.* (2010). Left-to-right atrial inward rectifier potassium current gradients in patients with paroxysmal versus chronic atrial fibrillation. Circ Arrhythm Electrophysiol 3: 472–480.

Wang L, Chiamvimonvat N, Duff HJ (1993). Interaction between selected sodium and potassium channel blockers in guinea pig papillary muscle. J Pharmacol Exp Ther 264: 1056–1062.

Wang Z, Yue L, White M, Pelletier G, Nattel S (1998). Differential distribution of inward rectifier potassium channel transcripts in human atrium versus ventricle. Circulation 98: 2422–2428.

Wenzler T, Yang S, Braissant O, Boykin DW, Brun R, Wang MZ (2013). Pharmacokinetics, Trypanosoma brucei gambiense efficacy, and time of drug action of DB829, a preclinical candidate for treatment of second-stage human African trypanosomiasis. Antimicrob Agents Chemother 57: 5330–5343.

Wijffels MC, Dorland R, Allessie MA (1999). Pharmacologic cardioversion of chronic atrial fibrillation in the goat by class IA, IC, and III drugs: a comparison between hydroquinidine, cibenzoline, flecainide, and d-sotalol. J Cardiovasc Electrophysiol 10: 178–193.

Wijffels MC, Kirchhof CJ, Dorland R, Allessie MA (1995). Atrial fibrillation begets atrial fibrillation. A study in awake chronically instrumented goats. Circulation 92: 1954–1968.

Wolf PA, Abbott RD, Kannel WB (1991). Atrial fibrillation as an independent risk factor for stroke: the Framingham Study. Stroke 22: 983–988.

Yang S, Wenzler T, Miller PN, Wu H, Boykin DW, Brun R *et al.* (2014). Pharmacokinetic comparison to determine the mechanisms underlying the differential efficacies of cationic diamidines against first- and second-stage human African trypanosomiasis. Antimicrob Agents Chemother 58: 4064–4074.

Yokoyama H, Nakamura Y, Iwasaki H, Nagayama Y, Hoshiai K, Mitsumori Y*et al.* (2009). Effects of acute intravenous administration of pentamidine, a typical hERG-trafficking inhibitor, on the cardiac repolarization process of halothane-anesthetized dogs. J Pharmacol Sci 110: 476–482.

Zeemering S, Maesen B, Nijs J, Lau DH, Granier M, Verheule S *et al.* (2012). Automated quantification of atrial fibrillation complexity by probabilistic electrogram analysis and fibrillation wave reconstruction. Conf Proc IEEE Eng Med Biol Soc 2012 (2012): 6357–6360.

Zhang H, Garratt CJ, Zhu J, Holden AV (2005). Role of up-regulation of I_{K1} in action potential shortening associated with atrial fibrillation in humans. Cardiovasc Res 66: 493–502.

Supporting Information

Additional Supporting Information may be found online in the supporting information tab for this article.

https://doi.org/10.1111/bph.13869

Data S1 Supplementary Methods.

Figure S1 Electrophysiological parameters in sinus rhythm dogs ($n = 4$) upon low dose bolus (0.5 mg.kg^{-1} 10 min^{-1}) (*A*) or high dose bolus (2.5 mg.kg^{-1} 10 min^{-1}) (*B*) up to 30 min following start of infusion. RR, PQ, QRS, QTc values are derived from ECG recordings. LV_{MAP80} and STVlv are derived from monophasic action potential recordings from the left ventricle.

Figure S2 Electrophysiological parameters in cAVB dogs ($n = 9$) upon high dose bolus (2.5 mg.kg^{-1} 10 min^{-1}) infusion up to 30 min following start of infusion. QRS and QTc values are derived from ECG recordings. LV_{MAP80} values are derived from monophasic action potential recordings from the left ventricle.

Figure S3 PA-6 mediated inhibition (50 and 200 nM) of human (Hs, *Homo sapiens*) and fish (Bb, *Blicca bjoerkna* (white bream)) $I_{Kir2.1}$ determined by patch-clamp electrophysiology in the inside-out orientation. Percentage amino acid sequence identity between Hs and Bb is 82.9%.

Figure S4 Amino acid alignment of human (Hs, *Homo sapiens*), dog (*Cf*, *Canis familiaris*) and goat (Ch, *Capra hircus*) $K_{ir}2.1$, $K_{ir}2.2$ and $K_{ir}2.3$ amino acid sequences in single letter code. Non-identical residues with respect to the human sequence are depicted in white font on a black background. Transmembrane region 1 and 2, selectivity filter, G-loop, Golgi and ER export signals are indicated in yellow. Blue shaded residues are involved in PA-6 mediated blockade. Genbank accession numbers and percentages of amino acid identity are given below the alignments.